Structure and Size of Spherical Micelles of Telechelic Polymers

Xiao-Xia Meng and William B. Russel*

Department of Chemical Engineering, Princeton University, Princeton, New Jersey 08544

Received May 25, 2004; Revised Manuscript Received November 5, 2004

ABSTRACT: This paper addresses the prediction and measurement of the aggregation number and radius of spherical micelles composed of telechelic polymers. The free energy of micellization balances the interfacial energy against the energy of stretching the end blocks to form the core, the configurational entropy, and excluded-volume interactions of the soluble chains that form the corona. In a good solvent, the latter are strongly stretched and form spherical brushes as treated by the Li−Witten model. The minimum in the free energy sets the most probable size, while the curvature at the minimum indicates the breadth of the distribution. From these we predict the various averages of the aggregation number and micellar radius detected by fluorescence measurements, dynamic and static light scattering, and viscometry. The effects of polydispersity explain in part the discrepancies among values reported by different groups for polymers of the same nominal structure.

1. Introduction

Telechelic associative polymers composed of hydrophilic backbones and hydrophobic ends self-assemble into micelles, which show some interesting and different solution properties relative to conventional small molecule surfactants. These are of interest because the aggregation profoundly affects macroscopic properties, for example, rheology. As with small surfactants, the hydrophobic ends aggregate to form a hydrophobic domain with the hydrophilic backbone extending into the solution to form a corona of soluble segments. Since the ends are usually much shorter than the backbone, spherical micelles always form. Distinct from small surfactants, the backbones of telechelic associative polymers are flexible and each backbone is capped on both ends. Hence, the interactions between the backbones differ from those between short chains. In addition, the ends from a telechelic polymer chain can exchange between the hydrophobic cores of interacting micelles to form a bridge. As a result of these differences, the aggregation number of telechelic polymers is usually much lower than that of small surfactants and the critical micelle concentration is less well-defined.

Various techniques have been employed to determine the aggregation number (number of polymer chains per micelle) and size of micelles. To detect the critical micellar concentration (cmc) and the aggregation number, p, Vorobyova et al.[1] and others monitor fluorescent probes, such as pyrene or its substituents, that partition strongly into hydrophobic domains. From the time-resolved fluorescent decay and the assumption that the quencher, which is the same as the probe in this case, follows a Poisson distribution in the micelles, they extract the mean number of quenchers per micelle. Vorobyova et al. reported the aggregation numbers of HDU-35 and ODU-35 (poly(ethylene oxide) of 35 kg/mol end-capped with hexadecyl and octadecyl groups, respectively) as 10.5 and 11.5, respectively. However, the values depend somewhat on the probe and strongly on the polymer concentration, prompting the authors to question the validity of the Poisson distribution, the effects of polydispersity, the formation of excimers, and the existence of oxygen impurities. When the cmc is not negligible, the probe also dissolves in the solution and produces a nonexponential decay.[2] In fact, the concentration of pyrene or its substituents was high and significantly affected the average aggregation number that emerged.[3−5] Neither could the authors account for self-quenching, which generates a two-exponential decay even in homogeneous solutions, nor a broad distribution of aggregation numbers, which can produce the strong dependence on the probe/polymer ratio. Others, such as Elliott et al., who employed static fluorescence with pyrene as the probe and benzophenone as the quencher, also observed concentration-dependent aggregation numbers.[6]

The aggregation number and radius of gyration of spherical micelles can be deduced from static light scattering either through a Zimm plot for dilute solutions or from detailed analysis of the structure and form factors in more concentrated solutions. Chassenieux et al.[7] examined a broad range of concentrations (from 0.01 to 10 wt %) for dodecyl-capped PEO with molecular weights 10, 20, and 35 kg/mol and observed a peak in scattering intensity as a function of scattering angle, which was ascribed to the coexistence of aggregates and unimers. Gourier et al.[8] attributed a similar peak in intensity that shifted with concentration to open association of micelles, from which they estimated the lower bound for the aggregation number. The traditional Zimm plot fails in both cases, leaving no unambiguous method for deducing the aggregation number and radius. Small-angle neutron scattering provides the same information as static light scattering but is capable of probing smaller length scales. Beaudoin et al.[9] assumed a simple cubic packing to calculate the aggregation number from the characteristic size indicated by the position of the main peak. Much similar work has been done with PEO end-capped fluoro-substituted hydrophobes. For example, Séréro et al. measured the aggregation number of micelles with $CF_3(CF_2)_8(CH_2)_{11}$ by small-angle neutron scattering.[10] More interestingly, they directly compared the telechelic polymer and a diblock equivalent to exactly half of the telechelic chain. Alternatively, Pham et al.[11] combined the hydrodynamic

* Corresponding author. E-mail wbrussel@princeton.edu.

10.1021/ma048968t CCC: $30.25
Published on Web 12/30/2004

radius of the micelles from dynamic light scattering with the intrinsic viscosity or specific hydrodynamic volume from capillary viscometry to estimate aggregation numbers. Unfortunately, the results from these different techniques usually disagree with each other. The aggregation number measured by static light scattering is slightly lower than from dynamic light scattering and viscometry, while the results from static fluorescence are lowest of all.[1,2]

The structure of associative polymers in a solvent selective for the backbone has attracted significant theoretical attention.[12−16] Scaling approaches developed for polymer brushes have been adopted to relate the aggregation number and cmc to the molecular structure by minimizing the free energy due to the interface formation, stretching of chains in the core, and interactions within the corona. Birshtein and Zhulina[14] and Halperin[15] et al. predicted the aggregation number to depend only on the hydrophobe size N_c as $p \sim N_c^{4/5}$ for hydrophilic blocks much larger than the hydrophobes. Nyrkova[16] also predicted a sole dependence on the hydrophobe size but as $p \sim N_c$. For surfactants with short PEO chains end-capped by alkanes, Nagarajan et al.[17] predicted aggregation numbers that decrease very quickly as the number of EO segments increases from a small number and level off for very long EO chains. Nagarajan's theory considered contributions to the free energy from the stretching of chains in the core, the interfacial energy, and the stretching and excluded volume from the corona. Since stretching a short chain is different from stretching a long chain, we do not expect the model to be accurate for polymers. Also, they assumed either the concentration in the corona to be uniform or the chains to be uniformly stretched. While reasonable when the corona is sufficiently thin for curvature to be unimportant, neither case is realistic for polymers. On the other hand, theory for polymers generally deals with diblocks, with both hydrophobic and hydrophilic parts polymeric. At the junction between them an interface with finite thickness forms to decrease the interfacial energy.[18] Recently, a theory proposed by Francois et al.[19] addressed the aggregation number and cmc of hydrophobically end-capped PEO by including energy penalties based on scaling arguments initiated by Daoud and Cotton and Zhulina. The theory explains qualitatively the effects of temperature and salt concentrations on micellization but is not quantitative because of the scaling arguments and does not account for polydispersity.

This paper is organized as follows. In section 2, we formulate a theory to predict aggregation number and the radius quantitatively, accounting for the polydispersity of both. In section 3, we compare the results from experiments of our group and others with the theory. Our predictions agree fairly well with experiments, with the polydispersity accounting for most of the discrepancies reported.

2. Theory

A micelle can be characterized nominally by two parameters: the radius and the aggregation number p. However, several radii can be defined theoretically or measured experimentally. In the Daoud−Cotton model,[12] all the arms in a micelle are stretched to the same extent so that all the ends reside at the edge, which defines a bounding sphere of radius R. By releasing the constraint of a stepwise distribution of the ends, the Li−Witten model[13] defined R as the largest distance the chain reaches from the core at equilibrium, which is larger than in the Daoud−Cotton model. Unfortunately, R cannot be measured directly. Static light and/or neutron scattering determines the radius of gyration R_g from the low-angle limit of the form factor. Alternatively, dynamic light scattering detects the hydrodynamic radius R_H as defined by the diffusion coefficient in dilute solutions. They are not expected to be the same since these radii characterize aspects of the micelle that weight the segment distribution differently. R_g represents the second moment of the segment distribution, while R_H reflects the cumulative effect of viscous drag on individual segments. In this paper, we assume R and R_H to be equal, which might be close for the following reasons. Certainly the corona of a micelle is partially permeable, making the hydrodynamic radius smaller than the maximum extension of the chain (or half chain in our case). However, thermal fluctuations allow a tail to reach beyond R, which increases R_H. The magnitude of the contributions from permeability and fluctuations are hard to evaluate, so we assume them to cancel. In this section, we formulate a theory to predict the dependence of the free energy on aggregation number and employ a Boltzmann distribution to characterize the probability of observing a particular aggregation number.

2.1. Predicting the Aggregation Number and Thermodynamic Radius. The aggregation number results from balancing interfacial energy, configurational entropy, and excluded-volume interactions in the corona against deformation energy of the hydrophobic chains in the core. In aqueous solutions, sufficiently small hydrophobes aggregate into a spherical core to minimize contact with water. If no water or hydrophilic segments penetrate the core, the hydrophobes form a pure organic liquid. Hence, we have a droplet of hydrophobes surrounded by a solution of hydrophilic chains. The interfacial region between the core and the solution allows contact between hydrophobes and water or hydrophilic segments, which contributes an interfacial energy but shields most of the hydrophobic ends from water. However, the segments at the center of the core belong to chains that must stretch inward from the interface, while the hydrophilic chains in the corona stretch toward the solution to reduce excluded-volume interactions near the interface. Nagarajan et al.[17] proposed a theory to predict the aggregation number for surfactants by accounting for the free energy of the stretching in the core, the formation of the interface, and the stretching and excluded volume of the EO chains. Although the stretching of a short EO chain differs from the stretching a polymer chain, the approach still holds for spherical micelles composed of telechelic polymers if the free energy of the corona is treated with a polymeric model. Li−Witten[13] searched for the minimum free energy for spherical brushes with respect to the trajectories of all polymer chains in configurational space by successively relaxing constraints on the end distribution, the local stretching function, and so on. This theory yields the free energy and radius of a micelle as a function of aggregation number p. The minimum free energy yields the most probable aggregation number, but thermal fluctuations produce a distribution of aggregation number around the most probable value. Hence, different average values result when weighted by number, weight, or other

factors, reflecting the polydispersity. For a broad distribution, the differences among the number, weight, z (from light scattering), and other average aggregation numbers can be significant.

The stretching energy per chain in the core is measured by the extent of stretching from the Gaussian end-to-end distance, $R_c/N_c^{1/2}l$, where R_c is the radius of the core, l is the length of a statistical segment, and N_c is the number of statistical segments in a hydrophobe. The free energy per chain due to the stretching in the core A_{core} scaled with thermal energy kT according to Nagarajan is thus[17]

$$\frac{A_{core}}{kT} = \frac{3\pi^2}{80}\frac{R_c^{\,2}}{N_c l^2} \tag{1}$$

R_c is related to p by a mass balance as

$$R_c = \left(\frac{3pN_c}{2\pi}\right)^{1/3} l \tag{2}$$

with each segment assumed to have volume l^3.

For a spherical micelle with $2p$ highly stretched arms of length N and a dimensionless excluded-volume parameter v, Li and Witten[13] found a region with radius r_c from which chain ends for diblocks, or midpoints for telechelics, are excluded. This radius is related to the radius of the micelle

$$R = 0.914(2pN^3v)^{1/5}l \tag{3}$$

through

$$r_c = 0.938R \tag{4}$$

The segment fraction $\varphi(r)$ at a distance r from the center takes different functional forms within and outside of the zone of exclusion

$$\varphi(r) = \begin{cases} 1.98N^{-2}v^{-1}(R^2 - r^2)l^{-2} & R > r > r_c \\ (r/r_c)^{-4/3}\varphi(r_c) & r_c > r \end{cases} \tag{5}$$

where

$$\varphi(r_c) = 0.198(2p)^{2/5}N^{-4/5}v^{-3/5} \tag{6}$$

with $r_c \gg R_c$. From these results they estimated the free energy per arm A_{corona} to be

$$\frac{A_{corona}}{kT} = 1.18((2p)^2v^2N)^{1/5} \tag{7}$$

Strictly speaking, the size of a unit of a hydrophobe is not the same as that of a hydrophilic chain, but the two l's happen to be very close for our model telechelic polymers, poly(ethylene oxide) (PEO) end-capped by alkanes. Chains are assumed to be strongly stretched, allowing a telechelic chain to be treated as two halves without affecting the free energy. Thus, a mixture of telechelic chains and half chains with the identical chemical structure should have the same aggregation number in terms of the number of hydrophobes per micelle, as shown by Laflèche et al.[20]

Calculating the interfacial energy, the product of the interfacial tension γ and the area of the interface a, is more complex. Since the interfacial tension between bulk phases of hydrophobes and solvent γ_{cs} differs from that between phases of hydrophobes and hydrophilic segments γ_{cp}, the hydrophilic chains are free to rearrange to minimize the interfacial energy. In other words, either the solvent or the hydrophilic segments could adsorb preferentially onto the interface, altering the composition. We account for this through the Prigogine theory, according to Siow et al.[21] and Nagarajan et al.,[17] which relates the bulk and interfacial concentrations by equating the corresponding chemical potentials. Hence, the interfacial concentration of the polymer φ_i depends on the adjacent bulk concentration φ_b (from the Li–Witten model), γ_{cp}, γ_{cs}, and the Flory interaction parameter between polymer and water $\chi = {}^1/_2(1 - v)$ as

$$\ln\frac{(\varphi_i/\varphi_b)^{1/N}}{(1-\varphi_i)/(1-\varphi_b)} = \frac{\gamma_{cs} - \gamma_{cp}}{kT}l^2 + \frac{3}{4}\chi(1 - 2\varphi_b) + \frac{1}{2}\chi(1 - 2\varphi_i) \tag{8}$$

The first term at right-hand side accounts for the interfacial energy due to the core–solvent and core–polymer contacts. The second term corrects for the polymer–solvent interaction. The interfacial tension γ follows from the interfacial tension between the hydrophobes and the solvent, modified due to the hydrophilic chains at the interface, as

$$\gamma = \gamma_{cs} + \frac{kT}{l^2}\left[\ln\frac{1-\varphi_i}{1-\varphi_b} - \frac{N-1}{N}(\varphi_i - \varphi_b) + \chi\left(\frac{1}{2}\varphi_i^{\,2} - \frac{3}{4}\varphi_b^{\,2}\right)\right] \tag{9}$$

When the interfacial tension of core–solvent contact is much higher than that of core–polymer, polymer segments adsorb onto the core to screen the direct interactions between the core and the solvent, which leads to a φ_i close to unity. In this case, the interfacial tension γ lies close to γ_{cp}. The interfacial energy per chain equals the interfacial tension times the contact area, which is the total area less that screened by chemically bonded chains:

$$\frac{A_{in}}{kT} = \frac{\gamma}{kT}(a - l^2) \tag{10}$$

where $a = 2\pi R_c^{\,2}/p$ characterizes the area per chain and l^2 is the area screened by each chemical bond. Equations 1, 7, 9, and 10 depend solely on p, given the structural parameters of the hydrophobes, the backbone, and the various interfacial tensions. At equilibrium

$$\frac{dA}{dp} \equiv \frac{d(A_{core} + A_{corona} + A_{in})}{dp} = 0 \tag{11}$$

determines the most probable aggregation number.

Because of thermal fluctuations, the aggregation number of individual micelles deviates from the most probable value, causing polydispersity. The probability $P(p)$ for a chain to belong to a micelle with an aggregation number p follows a Boltzmann distribution

$$P(p) = \frac{e^{-A/kT}}{\int_0^\infty e^{-A/kT}\,dp} \tag{12}$$

In a system with n_0 polymer chains per volume, the

number density of micelles containing p polymers $n_a(p)$ follows

$$n_a(p) = \frac{n_0 P(p)}{p} \tag{13}$$

From the distribution of p, several measurable aggregation numbers, namely, number-average p_n, weight-average p_w, and z-average p_z, can calculated as

$$p_n = \frac{\int_0^\infty p n_a(p)\, dp}{\int_0^\infty n_a(p)\, dp} \tag{14}$$

$$p_w = \frac{\int_0^\infty p^2 n_a(p)\, dp}{\int_0^\infty p n_a(p)\, dp} \tag{15}$$

$$p_z = \frac{\int_0^\infty p^3 n_a(p)\, dp}{\int_0^\infty p^2 n_a(p)\, dp} \tag{16}$$

Characterizing the polydispersity is essential for understanding discrepancies between measurements with different techniques.

2.2. Average of Selected Techniques. The weighting in the measurement of the aggregation number or radius depends on the technique employed. Here we examine the quantities measured by static light scattering, the combination of viscometry and dynamic light scattering, and fluorescence.

The radii measured by static and dynamic light scattering correspond to R_g and R_H, respectively. It is well-known that static light scattering yields a weight-averaged aggregation number (molecular weight) and a z-average of R_g from a Zimm plot,[22] whereas the combination of the dynamic light scattering and viscometry leads to a complex average of the aggregation number. We need to identify the average in each approach to compare to the theory.

In dilute solutions dynamic light scattering measures a z-average diffusion coefficient D_0, which determines a z-average reciprocal hydrodynamic radius R_H through the Stokes−Einstein equation

$$\frac{6\pi\mu\langle D_0\rangle_z}{kT} = \left\langle\frac{1}{R_H}\right\rangle_z = \frac{\int_0^\infty \frac{p^2 n_a(p)}{R_H}\, dp}{\int_0^\infty p^2 n_a(p)\, dp} \tag{17}$$

The hydrodynamic radius measured from dynamic light scattering follows as $1/\langle 1/R_H\rangle_z$.

When more than one technique is employed to determine the aggregation number, the weighting depends on that of each measured quantity. Pham et al.[11] assumed the hydrodynamic radius R_H from dynamic light scattering to apply for shear flows as well, allowing the intrinsic viscosity $[\eta]$, which is defined as $[\eta] = (\eta/\mu - 1)/c$ with η the viscosity of the polymer solution with concentration c and μ the viscosity of the solvent, to be expressed as $[\eta] = \{10\pi R_H^3 N_A\}/\{3pM\}$, with M the molecular weight of the polymer and N_A Avogadro's number for monodisperse micelles, such that

$$p = \frac{10\pi N_A R_H^{\,3}}{3M[\eta]} \tag{18}$$

With the knowledge of the weighting of R_H and $[\eta]$, the average of p from this approach, p_{d-v}, can be calculated.

The intrinsic viscosity characterizes the hydrodynamic volume of polymer chains; thus, for a distribution of micelles

$$[\eta] n_0 = 2.5 \int_0^\infty \frac{4\pi N_A}{3M} R_H^{\,3} n_a(p)\, dp \tag{19}$$

Relationships between R and R_H or R_g and R_H for various polymer architectures are available in the literature,[23] but are not immediately applicable to micelles. Therefore, we assume that $R = R_H$ as would be true for very large p, as discussed earlier.

Fluorescence is widely employed to detect the aggregation number of surfactants, and the effect of polydispersity is fairly well understood (cf. Gehlen and Schryver[5]). By monitoring the fluorescent decay $F(t)$ in a surfactant solution with probes and quenchers in the core of micelles, the kinetic constants and the aggregation number can be deduced from

$$F(t) = F(0)\exp[-t/\tau - N_q(1 - \exp(-k_q t)] \tag{20}$$

where $F(0)$ is the initial fluorescence intensity, t is the time, τ is the lifetime of an excited probe, N_q is the number of quenchers in a micelle, and k_q is the rate constant of the quenching process. To derive (20), quenchers are assumed to follow a Poisson distribution and not to escape from the micelles during the lifetime of an excited probe. The number of quenchers per micelle follows from the number densities of quenchers c_q and polymer chains c_p and the aggregation number p as

$$N_q = c_q p/c_p \tag{21}$$

The aggregation number deduced from eqs 20 and 21 is well-defined for monodisperse micelles. However, the average of the aggregation number of polydisperse micelles depends on the relative lifetimes of a micelle and an excited probe. When the lifetime of a micelle is much shorter than the residence time of a probe, the process is "dynamic" in the sense that a probe samples micelles of all sizes during its lifetime, and the aggregation number from fitting the fluorescent decay curve is always number-averaged, regardless of the concentration of the quencher. On the other hand, when the lifetime of a micelle is longer than the residence time of a probe, defined as a "static" process, the average aggregation number depends on the concentration of the quencher, approaching the weight-average in the limit of zero quencher concentration.[3,4] In the static limit, the aggregation number $\langle p\rangle_Q$ is averaged by the ratio of the concentrations of the quencher to the hydrophobe as follows:[4]

$$\langle p\rangle_Q = \frac{p}{N_q} \ln \frac{\sum_p p n_a(p)}{\sum_p p \exp(-N_q p)\, n_a(p)} \tag{22}$$

When the distribution of the aggregation number is known, eq 22 can be expanded to a power series in N_q

Table 1. Parameters To Calculate the Aggregation Number and Radius

l (nm)	l_p (nm)	v	n_c	n_E	σ_c (mN/m)	σ_s (mN/m)	σ_p (mN/m)
0.455	0.456	0.3	16−18	63−400	26.3−26.9	72	41.3−42.1

and represented in terms of the ith moments of the aggregation number p_i

$$\langle p\rangle_Q = \frac{p_2}{p_1} - \frac{1}{2}\left[\frac{p_3}{p_1} - \left(\frac{p_2}{p_1}\right)^2\right]\frac{N_q}{p} + O\left(\frac{N_q}{p}\right)^2$$
$$= p_w - \frac{1}{2}[p_z - p_w]p_w\frac{N_q}{p} + O\left(\frac{N_q}{p}\right)^2 \qquad (23)$$

When the quenching is fast so that the micelles are essentially frozen, the quencher average aggregation number approaches the weight-average as the concentration of the quencher approaches zero.[4] A relatively low quencher concentration is preferred because it avoids the higher-order terms in the concentration dependence of the aggregation number and minimizes the perturbation to the core size and the quenching from the continuous phase as well.

Static fluorescence imposes a continuous excitation and measures the intensity of the fluorescence as a function of the concentration of the quencher. If observed long enough, micelles around a particular quencher fluctuate during the measurement and sample all the configurations, so the Poisson distribution of quenchers does not depend on the size of micelles, as in the case of "dynamic" limit of the dynamic fluorescence discussed above. Hence, we think that the aggregation number is the number-average in static fluorescence. Indeed, people have observed the aggregation number measured from static fluorescence to be systematically smaller than that from dynamic fluorescence.[24]

So far, with the knowledge of the molecular structure the surface tension data of the hydrophobes and backbones, we can predict the aggregation number and the radius of the micelle from understanding of the energetics of the system.

3. Experiments

3.1. Materials. Synthesis of HDU-20, HDU-35, and ODU-35 at Rohm and Haas followed the procedure reported by Pham et al.[11] Gel permeation chromatography showed a polydispersity less than 1.2 for both PEO backbones, and reversed phase liquid chromatography indicated >95% of the chain ends to be capped with hydrophobes for HDU-20 and HDU-35, while ODU-35 was fully end-capped. HDU-35 and ODU-35 were dissolved in a mixed solvent of water/acetone to obtain a solution with a concentration of 10 wt % and filtered through 0.2 μm Millipore syringe filters to remove water-insoluble impurities. Then the solvent was removed by purging with filtered nitrogen overnight. All the samples were then prepared by dissolving the purified polymers in double distilled water. HDU-20 was dissolved in double distilled water first and then filtered with Millipore filters. All samples were mixed overnight before experiments.

3.2. Dynamic Light Scattering (DLS). Dynamic light scattering was performed at an angle of 90° and 25 °C on a light scattering instrument with a Brookhaven goniometer, an ALV-5000 multiple decay time correlator, and an argon ion laser with wavelength of 514.5 nm. All the measurements were performed at concentrations below the lower phase boundary, i.e., <2000 ppm for all polymers.[11]

3.3. Viscometry. HDU-20 was dissolved in double distilled water and mixed overnight to obtain dilute solutions of 200−1500 ppm. Viscosity was measured by a Ubbelohde viscometer controlled by a Scott-Gerate AVS 360 equipped with a 531 01/0a capillary (diameter 0.53 mm). The flow was driven solely by gravity, which ensured a shear rate about 100 s^{-1} during the measurement. The Hagenbach correction was included to account for inertia.

4. Results and Discussion

With our theory we calculate the aggregation number and the size of micelles for a family of popular telechelic associative polymers, PEO end-capped with dodecyl, octadecyl, or hexadecyl hydrophobes, and compare the results with available data from fluorescence, dynamic and light scattering, and viscometry. First, however, we need the parameters that characterize the molecular structure of the telechelic polymers to complement the surface tension and microscopic sizes available from Nagarajan et al.[17]

The number of statistical segments in both the hydrophobes and the hydrophilic backbones depends on the number of units and the flexibility of the chains. Although flexible on the large scale, the chains are stiff within a few bonds. Hence, we need to know the maximum number of units for which the stiffness still affects the configurations. For alkanes, the monomer units feel each other only through excluded volume after 3.6 CH_2's.[17] Since a CH_3 group is twice as big as a CH_2 group, the number of characteristic segments is $N_c = (n_c + 1)/3.6$, where n_c is the number of carbon atoms in a hydrophobe. Another way of evaluating N_c is to calculate the length of a stretched hydrophobe by summing up the group contributions from CH_2 and CH_3. The total length of an alkane chain is $l_c = 0.15 + 0.1265n_c$ (nm),[17] so $N_c = l_c/l$ and 3.6 CH_2 units have a length of $l = 0.455$ nm.[17] The length of a PEO statistical segment, which consists of 3.8 bonds, is 0.455 nm,[11] so we treat the hydrophobic and hydrophilic segments as indistinguishable. Hence, the number of statistical segments in a half chain is $N = 3n_E/3.8$, with n_E the number of EO units, each of which contributes three bonds.

The surface tensions against air of both hydrophobes and PEO decrease with increasing size of the block as $\sigma_c = 35 - 56n_c^{-2/3}$ mN/m and $\sigma_p = 42.5 - 19n_E^{-2/3}$ mN/m at 298 K.[17] The interfacial tensions between the condensed phases can be estimated from the surface tension of each component σ_i (i = c, hydrophobe; i = p, polymer; i = s, solvent) as[17]

$$\gamma_{cs} = \sigma_c + \sigma_s - 1.1(\sigma_c\sigma_s)^{1/2} \qquad (24)$$

for a water−alkane interface and

$$\gamma_{cp} = \sigma_c + \sigma_p - 1.1(\sigma_c\sigma_p)^{1/2} \qquad (25)$$

for a PEO−alkane interface. The numerical factors are taken to be equal because the interactions between EO's and hydrophobes are very similar to those between water and hydrophobes. The excluded-volume parameter in eq 7 was taken to be 0.3, in the rather wide range from experimental data $v/l^3 = 0.15-1.1$.[11] All the parameters are summarized in Table 1.

With eqs 1, 2, and 7−10, we minimize the free energy with respect to p to determine the most probable aggregation number and then determine the radius of

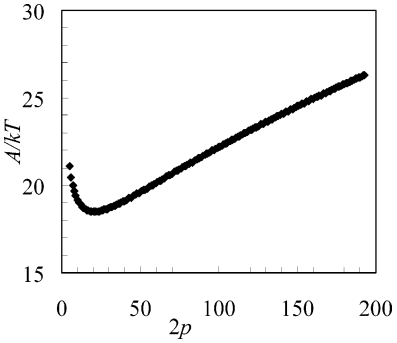

Figure 1. Free energy vs number of hydrophobes in the core for HDU-35.

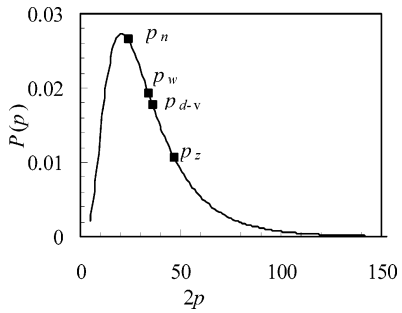

Figure 2. Distribution of the number of arms in a micelle (HDU-35) with symbols indicating averages with various weights.

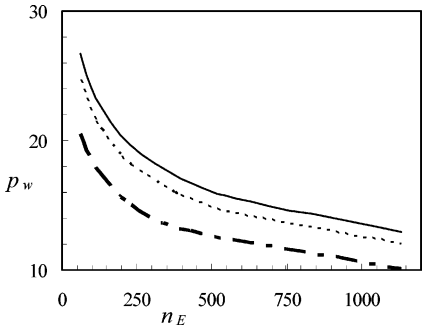

Figure 3. Weight-average aggregation number of telechelic polymers with hydrophobes C_{12} (— · —), C_{16} (· · ·), and C_{18} (—).

the micelles R from eq 3. Figure 1 shows the relationship between free energy and the aggregation number. Close to the minimum, thermal fluctuations of $O(kT)$ can change the aggregation number from the most probable value of 9.3 to $4 \leq p \leq 23$ for HDU-35, indicating that the micelles should be fairly polydisperse. This becomes more obvious in Figure 2, which displays the probability $P(p)$ vs p and identifies the three different average aggregation numbers with $p_z > p_w \approx p_{d-v} > p_n$. Predictions of the weight-average aggregation number and the radius for telechelic polymers end-capped with $C_{12}H_{25}$, $C_{16}H_{33}$, and $C_{18}H_{37}$ are plotted as a function of the number of EO segments n_E in Figures 3 and 4, respectively. When the molecular weight of the PEO block is low, the aggregation number and the radius are sensitive to n_E. When the PEO block is large so that it screens the hydrophobes effectively from water, the aggregation number and radius become less sensitive to molecular weight.

In Figure 5a, we compare our predictions with the p measured by various groups. The predictions of the number-average aggregation number agree well with static fluorescence data by Alami et al. and Elliot et al.[6,24] In very dilute polymer solutions, the ratio of polymer/micelle to the probe and quencher is low. The probe and quencher might induce aggregation or change the aggregation number due to a significant contribution to the volume of the hydrophobic domain. To minimize these effects, we take only the high polymer concentration values, where the aggregation number approaches a plateau.

Dynamic fluorescence measures the aggregation number by fitting the fluorescent decay to a Poisson distribution of quenchers and leads to weight-average aggregation numbers at zero quencher concentration limit. Figure 5b shows a fairly good agreement between the predicted and measured weight-average aggregation numbers by Alumi et al.[24] and Yekta et al.[25] The HEUR might not be fully end-capped by the hydrophobes, so Yekta et al. took this effect into account by characterizing the number of hydrophobes with NMR. Effects of polydispersity did not seem to be a problem in their case since the aggregation number did not vary with the ratio

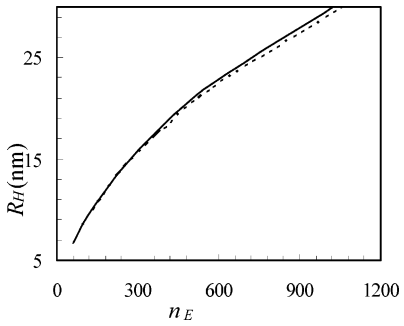

Figure 4. Radius of the micelles with telechelic polymers end-capped by C_{16} (· · ·) and C_{18} (—).

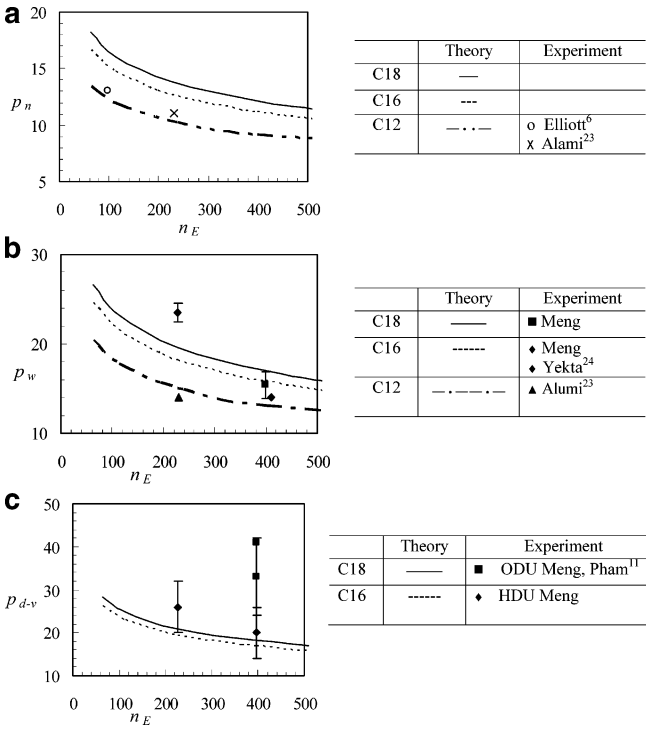

Figure 5. (a) Predicted vs experimental number-average aggregation numbers with lines and symbols in the figure. (b) Predicted vs experimental weight-average aggregation number with lines and symbols defined as in the figure. (c) Predicted vs experimental aggregation number by dynamic light scattering and viscometry with lines and symbols defined as in the figure.

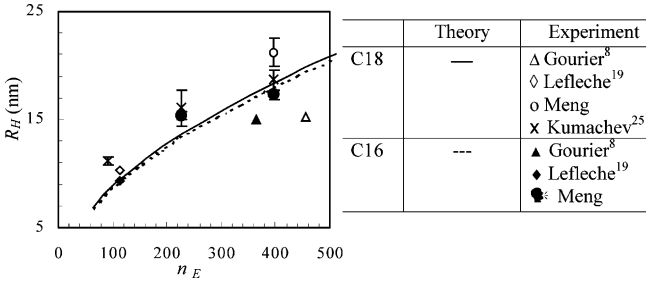

Figure 6. Predicted vs experimental radius of micelles, averaged as in eq 19 with lines and symbols defined as in the figure.

of probes/quenchers to polymer chains. In measurements by Alumi et al., though, the aggregation number did change with the concentration of the polymer, but without any reasonable trends. Other dynamic fluorescence data from Vorobyova et al.[1,2] were not included since the quencher concentration employed was very high, and it is unclear to us what average results from their analysis. Our measurements of aggregation number from static light scattering also yield weight-average aggregation numbers consistent with the predictions. We only included the data that produced reasonable straight lines on a Zimm plot, excluding the data for HDU-35 that showed strong curvature.

From the dynamic light scattering and viscometry, the p_{d-v} determined from eqs 17−19 are lower than the aggregation numbers measured by the combination of dynamic light scattering and viscometry, which could be ascribed to uncertainties in the measurements of the radius and intrinsic viscosity as indicated by the error bars and differences from Pham's[11] and our measurements on ODU-35 with the same instrument under the same conditions. Because the aggregation number depends on the cube of hydrodynamic radius, the error in the radius is magnified in the aggregation number. The uncertainty of the relation between R and R_H could explain the systematic deviation we observe in Figure 6, and thus Figure 5c, which assumed the two radii to be identical.

The reciprocal of the z-average $1/R$ of the micelles agrees well with the hydrodynamic radius measured by dynamic light scattering from a few groups on a variety of model telechelic associative polymers,[11,26] as shown in Figure 6. It is worth noting that even though the aggregation number varies dramatically with techniques and polymer identities, the radii compare with the predictions fairly well, partially because of the weak radius dependence (1/5 power) on the aggregation number.

Both scattering and fluorescence detect a concentration-dependent aggregation number, as Elliott et al. observed,[6] which might arise from screening of the excluded volume at high concentrations. This is qualitatively consistent with the increase in the aggregation number for ODU-35 as the excluded-volume parameter decreases in Figure 7.

Another important trend that emerges from our theory is the dependence of the aggregation number on both the hydrophobe size and the molecular weight of the backbone, contrary to predictions in the literature.[15,16] At a fixed molecular weight of the backbone, our expectation that $p \sim N_c^{4/5}$(from Figure 8) conforms with predictions of Zhulina et al.[14] and Halperin et al.[15] Admittedly, the dependence on the backbone size is weak ($p \sim N^{-1/5}$), though not always negligible.

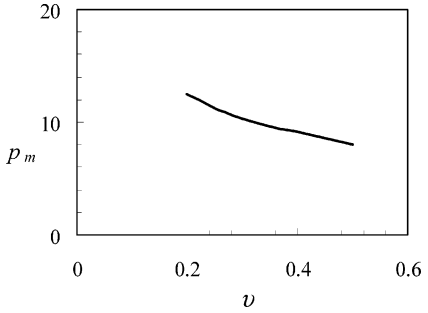

Figure 7. Most probable aggregation number decreases with increasing excluded volume for ODU-35.

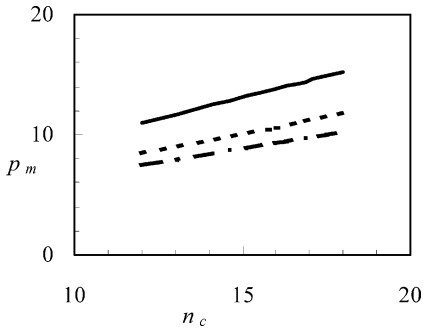

Figure 8. Aggregation number vs number of CH_2 in the hydrophobes: EO 63 (—), EO 20K (- - -), and EO 35K (— · —).

5. Conclusions

This paper describes a theory to predict the aggregation number and radius of the micelles from the molecular structure and a few parameters, such as the surface tensions of the hydrophobic and hydrophilic blocks of the polymer and the solvent, available elsewhere in the literature. The aggregation number is an equilibrium property determined by the free energy of the micelle. We calculate contributions to the free energy from the interface, stretching of chains, and excluded-volume interactions through models from Nagarajan for the core and interfacial energies and Li and Witten for the corona. Minimizing the free energy determines the most probable aggregation number, while the variation about the minimum yields the distribution of the aggregation numbers, from which p_n, p_w, and p_z can be calculated. The corresponding radii follow from the Li−Witten model.

We compare our predictions with measurements by various techniques. The predicted number-average aggregation numbers agree well with fluorescence data. Our prediction of the z-average $\langle 1/R \rangle$ is consistent with dynamic light scattering. Predictions of aggregation number from eqs 17−19 are lower than those determined by dynamic light scattering and viscometry. Nonetheless, our predictions conform reasonably well on the whole with data in the literature.

However, there are still data in the literature that we cannot compare with theory. Vorobyova et al.[1,2] extracted aggregation numbers of HDU-35 and ODU-35 from dynamic fluorescence, for which the nature of the average that results from their analysis remains unclear. Likewise, the SANS data by Beaudoin et al.[9] are also interesting, but the weighting factor in this average is hard to judge. Although the theory here applies to other type of polymers such as polymers endcapped with fluoro-substituted hydrophobes, the absence of value for parameters characterizating these

hydrophobes prohibits us from predicting the aggregation numbers and comparing to experiments.

Acknowledgment. The authors appreciate the support from NSF (Division of Engineering Chemical and Transport Systems) through Grants CTS: 98-12409 and CTS01-20421. Also, we are grateful for the generous supply of polymers from Dr. Willie Lau in Rohm and Haas and Sharon X. Ma from University of Delaware. X.M. also thanks Dr. Winnik and Dr. Kumacheva for sharing data and helpful discussions.

References and Notes

(1) Vorobyova, O.; Yekta, A.; Winnik, M. A.; Lau, W. *Macromolecules* **1998**, *31*, 8998.
(2) Vorobyova, O.; Lau, W.; Winnik, M. A. *Langmuir* **2001**, *17*, 1357.
(3) Warr, G. G.; Grieser, F. *J. Chem. Soc., Faraday Trans. 1* **1986**, *82*, 1813.
(4) Almgren, M.; Lofroth, J.-E. *J. Chem. Phys.* **1982**, *76*, 2734.
(5) Gehlen, M. H.; Schryver, F. C. D. *Chem. Rev.* **1993**, *93*, 199.
(6) Elliott, P. T.; Xing, L.-L.; Wetzel, W. H.; Glass, J. E. *Macromolecules* **2003**, *36*, 8449.
(7) Chassenieux, C.; Nicolai, T.; Durand, D. *Macromolecules* **1997**, *30*, 4952.
(8) Gourier, C.; Beaudoin, E.; Duval, M.; Sarazin, D.; Maitre, S.; François, J. *J. Colloid Interface Sci.* **2000**, *230*, 41.
(9) Beaudoin, E.; Borisov, O.; Lapp, A.; Billon, L.; Hiorns, R. C.; François, J. *Macromolecules* **2002**, *35*, 7436.
(10) Séréro, Y.; Aznar, R.; Porte, G.; Berret, J.-F.; Calvet, D.; Collet, A.; Viguier, M. *Phys. Rev. Lett.* **1998**, *81*, 5584.
(11) Pham, Q. T.; Russel, W. B.; Thibeault, J. C.; Lau, W. *Macromolecules* **1999**, *32*, 2996.
(12) Daoud, M.; Cotton, J. P. *J. Phys. (Paris)* **1982**, *43*, 531.
(13) Li, H.; Witten, T. A. *Macromolecules* **1994**, *27*, 449.
(14) Birshtein, T. M.; Zhulina, E. B. *Polymer* **1989**, *30*, 170.
(15) Halperin, A. *Macromolecules* **1987**, *20*, 2943.
(16) Nyrkova, A.; Khokhlov, A. R.; Doi, M. *Macromolecules* **1993**, *26*, 3601.
(17) Nagarajan, R.; Ruckenstein, E. *Langmuir* **1991**, *7*, 2934.
(18) Broseta, D.; Leibler, L. *J. Chem. Phys.* **1987**, *87*, 7248.
(19) Francois, J.; Beaudoin, E.; Borisov, O. *Langmuir* **2003**, *19*, 10011.
(20) Laflèche, F.; Durand, D.; Nicolai, T. *Macromolecules* **2003**, *36*, 1331.
(21) Siow, K. S.; Patterson, D. *J. Phys. Chem.* **1973**, *77*, 356.
(22) Kerker, M. *The Scattering of Light and Other Electromagnetic Radiation*; Academic Press: New York, 1969.
(23) Grest, G. S.; Fetters, L. J.; Huang, J.; Richter, D. In *Advances in Chemical Physics*; Prigogine, I., Rice, S. A., Eds.; John Wiley & Sons: New York, 1996; Vol. XCIV, pp 67−163.
(24) Alami, E.; Almgren, M.; Brown, W.; Francois, J. *Macromolecules* **1996**, *29*, 2229.
(25) Yekta, A.; Xu, B.; Duhamel, J.; Adiwidjaja, H.; Winnik, M. *Macromolecules* **1995**, *28*, 956.
(26) Kumacheva, E., personal communication.

MA048968T